A Method for the Simulation of Powder Electron Spin Resonance Spectra when $S > \frac{1}{2}$; Application to the Iron–Molybdenum–Sulphur Protein of Nitrogenase and of Some $[Fe_4S_4(SR)_4]^{3-}$ Clusters

By **David Collison** and **Frank E. Mabbs,*** Chemistry Department, University of Manchester, Manchester M13 9PL

A method for simulating powder e.s.r. spectra of systems with $S > \frac{1}{2}$ in the absence of hyperfine interactions is described. The method involves diagonalisation of the spin-Hamiltonian matrix, curve-fitting the resulting energies to obtain the resonance fields, calculating the transition probabilities of the resonances, and weighting the energy states from which transitions are being stimulated according to their relative thermal occupation. The simulation process is applied to published e.s.r. spectra of the FeMo protein and FeMo cofactor from *Azotobacter vinelandii* and *Clostridium pasteurianum*, and to the powder spectra of $[NR'_4]_3[Fe_4S_4(SR)_4]$ (where R' = Pr^n, R = $CH_2C_6H_5$; R' = Et, R = $CH_2C_6H_5$ or $CH_2C_6H_4OMe$-*p*; and R' = Me, R = C_6H_4Me-*p*).

THE frozen glass or powder e.s.r. spectra of iron–sulphur,[1] iron–molybdenum–sulphur [2] proteins, and synthetic analogues of such proteins,[1-6] are sometimes complex. The appearance of these e.s.r. spectra are often indicative of the presence of paramagnetic centres with $S > \frac{1}{2}$. The extraction of spin-Hamiltonian parameters from such spectra, or indeed the confirmation of the particular choice of the value of S, is not necessarily simple, since the powder spectra may include resonances which occur when the applied magnetic field is at orientations other than those parallel to the molecular axes.[7-9] Thus in order reliably to interpret powder e.s.r. spectra it is essential to simulate them.

The simulation of e.s.r. spectra requires a knowledge of the variation of the eigenvalues and eigenvectors of the components of the spin, S, with the magnitude and direction of the applied magnetic field. For $S > \frac{1}{2}$ this information is not generally available as closed form expressions [10,11] or in terms of effective parameters.[12] Thus, *e.g.* when $S = 1$ or $\frac{3}{2}$, closed form expressions are available for any values of g, D, and E only when the applied magnetic field is parallel to the molecular axes.[11] These relationships would allow prominent features only to be accounted for in a powder e.s.r. spectrum. Under the conditions that $g\beta_e H \gg D$ or $g\beta_e H \ll D$, perturbation theory may be used to obtain closed form expressions for the angular variation of the resonance fields for $\Delta M_s = \pm 1$ transitions, thereby facilitating spectrum simulation.[8,10,11,13-18] When these conditions are not satisfied then exact solutions *via* matrix diagonalisation must be used. This approach to the interpretation of $S > \frac{1}{2}$ powder or frozen glass spectra has been discussed.[7,9,18,19] However, these discussions are mainly concerned with predicting the major features in the spectrum when the applied magnetic field is parallel to the principal axes rather than simulating the whole spectrum,[7-9,14-19] although complete simulations are reported for some $S = \frac{5}{2}$ systems with the restriction to axial symmetry.[20]

During the course of our investigations of the e.s.r. behaviour of synthetic analogues of iron–sulphur and of iron–molybdenum–sulphur proteins, we have discerned the need to simulate the e.s.r. spectra of systems with $S > \frac{1}{2}$ when we cannot make any assumptions concerning either the symmetry or the relative magnitudes of the various perturbations present. Thus we wish to report a method for the simulation of powder e.s.r. spectra under these conditions, and its application to the available spectra on the iron–molybdenum protein, the iron–molybdenum co-factor of *Azobacter vinelandii*, and of *Clostridium pasteurianum*.[2] The powder e.s.r. spectra of the synthetic cubane cluster compounds [3] $[NR'_4]_3[Fe_4S_4(SR)_4]$, where R' = Pr^n, R = $CH_2C_6H_5$; R' = Et, R = $CH_2C_6H_5$ or $CH_2C_6H_4OMe$-*p*; R' = Me, R = C_6H_4Me-*p*, are also simulated.

EXPERIMENTAL

Method of Spectrum Simulation.—It is assumed that the principal axes of the g and zero-field splitting tensors are coincident with each other and with the molecular axes. In these circumstances the simulation of a powder or frozen glass e.s.r. spectrum may be treated as a sum of randomly oriented molecules, but with the advantage that the calculation can be confined to a single octant of spherical space.[21]

A general spin-Hamiltonian, for any $S > \frac{1}{2}$, without hyperfine interaction, may be written as equation (1), where θ and ϕ are the polar angles of the applied magnetic field, H, with respect to the molecular axes. Since in general we

$$\mathcal{H} = \beta_e[g_z H\cos\theta \hat{S}_z + \tfrac{1}{2}g_x H\sin\theta\cos\phi(\hat{S}_+ + \hat{S}_-) - \frac{\sqrt{-1}}{2} g_y H\sin\theta\sin\phi(\hat{S}_+ - \hat{S}_-)] + D[\hat{S}_z^2 - \tfrac{1}{3}S(S+1)] + \tfrac{1}{2}E[\hat{S}_+\hat{S}_+ + \hat{S}_-\hat{S}_-] \quad (1)$$

do not wish to make any assumptions concerning the relative magnitudes of the Zeeman or zero-field splitting effects we require the solution to the secular determinant arising from the application of equation (1) to the $2S + 1$ spin components defined as $|M_s>$. For a field-swept e.s.r. experiment the variation of the energy levels $\varepsilon_i(\theta,\phi,H)$ with applied magnetic field is required so that the resonance condition [equation (2)] can be examined, where ν = applied

$$\varepsilon_j(\theta,\phi,H) - \varepsilon_i(\theta,\phi,H) = h\nu \quad (2)$$

microwave frequency. In the absence of general analytical expressions for the variation of energy levels with θ, ϕ, H, g, D,

and E, for $S > \frac{1}{2}$, we obtain the information required for the application of equation (2) by the following curve-fitting procedure. For a given set of spin-Hamiltonian parameters we diagonalise the secular determinant at each orientation of the applied magnetic field at a number of magnetic fields, H_n, separated by intervals ΔH. This is achieved by using the Nottingham Algorithms Group library eigenvalues routine FO2AWF on the University of Manchester Regional Computer Centre ICL 1900/CDC7600 Joint System to yield a set of eigenvalues $\varepsilon_i(\theta,\phi,H_n)$ in ascending order of energy. At a fixed value of the magnetic field the energy difference between the ith and jth levels compared to the applied microwave energy gives the variable $\Delta\varepsilon(H_n)$ in equation (3). The

$$\Delta\varepsilon(H_n) = \varepsilon_j(\theta,\phi,H_n) - \varepsilon_i(\theta,\phi,H_n) - h\nu \qquad (3)$$

quantity $\Delta\varepsilon(H_n)$ for the same pair of i and j at different values of H_n was then fitted to a polynomial in H_n using the Chebyshev series representation.[22] The value of H_n for which $\Delta\varepsilon(H_n) = 0$ was then determined by numerical interpolation of the above polynomial using small magnetic field intervals δH. The curve-fitting and interpolation were accomplished using the computer routines EO2AFF and EO2AEF. At this stage it does not matter that there may have been crossing of the energy levels as the magnetic field varied, since eventually the probability of the proposed transition was calculated. The value of the magnetic field at which equation (2) is satisfied was substituted into the energy matrix resulting from equation (1) and the matrix rediagonalised to yield the appropriate eigenvalues and eigenvectors, $\phi_i = \sum_{k=1}^{2S+1} c_k|M_{s_k}\rangle$, using the computer routine FO2AXF. The probability, P_i, for the proposed transition was then calculated [23] from equation (4), where $\eta_{osc.}$ is

$$P_i = |\langle \phi i \,|\, \eta_{osc.} g.\hat{S} \,|\, \phi_j \rangle|^2 \qquad (4)$$

the unit vector of the microwave field. The above procedure was repeated for all pairs of energy levels. In this way the magnetic fields at which transitions could occur, and their associated transition probabilities, were separately stored for the whole range of magnetic fields and angles.

In many instances spectra are obtained over a wide range of temperatures, especially at liquid helium temperatures. The differential thermal population of the levels from which transitions were being stimulated was considered by assuming a Boltzmann distribution over the energy levels $\varepsilon_i(\theta,\phi,H)$. Thus the transition probabilities were weighted by C_i in equation (5), where C_i = weighting for the ith level from

$$C_i = e^{-(\varepsilon_i/kT)} / \sum_{\text{all } S} \sum_{k=1}^{2S+1} e^{-(\varepsilon_k/kT)} \qquad (5)$$

which the transition occurs, and ε_j is with respect to the lowest energy level for all S states (at the particular θ, ϕ, and H) being defined as zero.

The simulation of a spectrum of a powder or frozen glass proceeded by choosing orientations which defined approximately equal surface areas throughout an octant,[21] using $d\phi(\theta) = d\theta/\sin\theta$, for $\theta \neq 0$. The spectrum for a rhombic system is thus a sum of spectra obtained from all of these orientations. In an axially symmetric case, although the spectrum does not change with ϕ, the number of ϕ angular contributions must be considered. This was achieved by weighting the transition probability at each value of θ by $[90/d\phi(\theta)] + 1$ for $d\phi(\theta) \neq 0$.

The contribution to the first derivative spectrum from each individual transition was calculated using the closed form equation (6), assuming a Gaussian lineshape function, where $(TP)_i$ is the transition probability weighted for thermal population, the number of times, η, a particular S occurs at the same energy, and ϕ angular contributions

$$\left(\frac{dI}{dH}\right)_i = \left(\frac{1}{\Delta B}\right)^3 (TP)_i (H_{app.} - H_{res.}) \exp\left[-\frac{2(H_{app.} - H_{res.})^2}{(\Delta B)^2}\right] \qquad (6)$$

where appropriate. In addition $H_{app.}$ is the applied magnetic field, $H_{res.}$ the magnetic field for resonance, ΔB the effective linewidth which is related to the molecular linewidths W_i by equation (7).

$$\Delta B = (W_x^2\sin^2\theta\cos^2\phi + W_y^2\sin^2\theta\sin^2\phi + W_z^2\cos^2\theta)^{\frac{1}{2}} \qquad (7)$$

The contribution from each transition was truncated for $H_{app.}$ more than $\pm 3\Delta B$ from $H_{res.}$. The total first derivative spectrum, TS, was then obtained from equation (8),

$$TS = \sum_{i=1}^{l} \sum_{m} \left(\frac{dI}{dH}\right)_i \qquad (8)$$

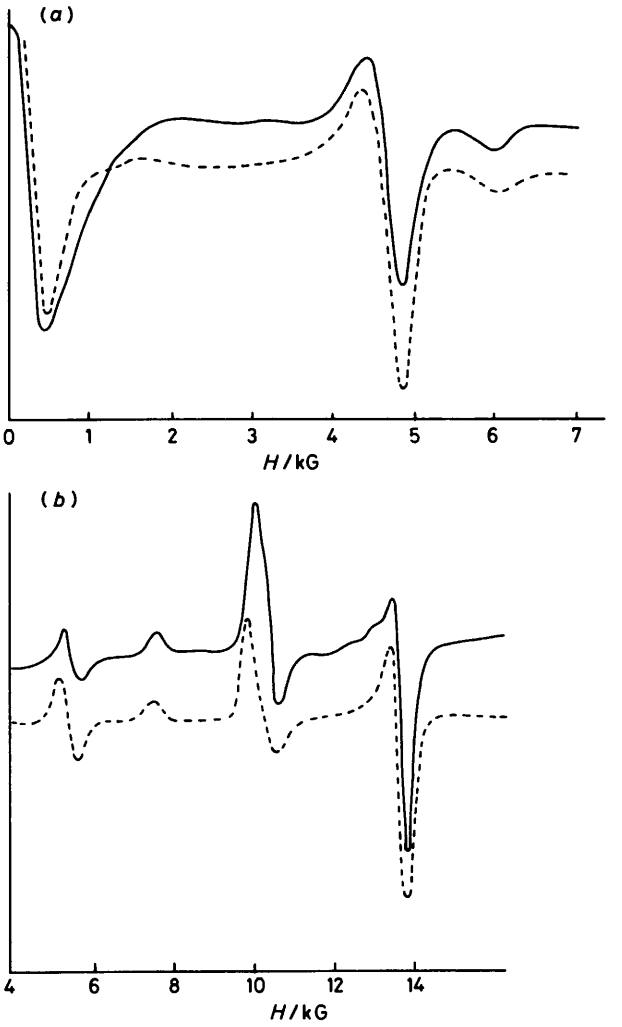

FIGURE 1 Experimental (this work) and simulated room temperature e.s.r. spectra of $[\{Cu(O_2CMe)_2(H_2O)\}_2]$. Spectra simulated with $g_z = 2.344$, $g_x = 2.053$, $g_y = 2.093$, $D = 0.345$ cm^{-1}, $E = 0.01$ cm^{-1}, $W_z = W_x = 400$, $W_y = 250$ G, $d\theta = 3°$: (*a*) $\nu = 9.492$ GHz; and (*b*) $\nu = 34.992$ GHz

where l is the total number of transitions and m is the number of applied magnetic field points each separated by $\Delta H_{app.}$.

The final calculated spectrum was displayed graphically on a Benson narrow-drum graph plotter using the GHOST graph-plotting routines on the University of Manchester Regional Computer.

RESULTS AND DISCUSSION

The accuracy and successful application of this method for simulating powder spectra, without involving excessive computation times, depends upon an appropriate choice of the curve-fitting variables and of dθ. In the curve-fitting procedure the accuracy of the resonance positions has been checked against those calculated where analytical expressions are available. In all cases we have found that our calculated resonance fields, compared to those from the analytical expressions, have a maximum error equal to the magnetic field interval used in the interpolation process. It is possible in the curve-fitting procedure that some resonances may be overlooked by an inappropriately large value of ΔH. This can always be checked by noting the effect of reducing ΔH on the computed spectrum. Our experience with the method indicates that $\Delta H = 200$ G * is a suitable choice for the systems reported here. We have not found any situation where resonances have been overlooked.

The choice of dθ is particularly important in terms of computation time, since this determines the number of matrix diagonalisations which have to be performed. Thus a value of dθ as large as possible should be chosen. Our empirical observations are that the maximum value of dθ is determined by the linewidths of the transitions *versus* the shift of the resonance position with angle. If the resonance field changes with dθ by more than the linewidth then spurious features appear in the simulated spectrum. Such spurious features result in spectra which resemble those obtained from incompletely randomly oriented crystallites and are readily recognised. When this occurs then dθ must be reduced to eliminate this effect.

An example of the comparison between simulated and experimental spectra for which the spin-Hamiltonian parameters have been determined from single-crystal studies is that of bis[bis(acetato)aquacopper(II)],[24] Figure 1. In this compound the spectrum arises from a $S = 1$ system with rhombic symmetry. The broad linewidths required in this room temperature spectrum are assumed to arise mainly from unresolved copper hyperfine interactions. The simulated and experimental spectra at both X- and Q-band frequencies are in good agreement. The spin Hamiltonian parameters used to simulate the spectra were those reported from the single-crystal study.[24]

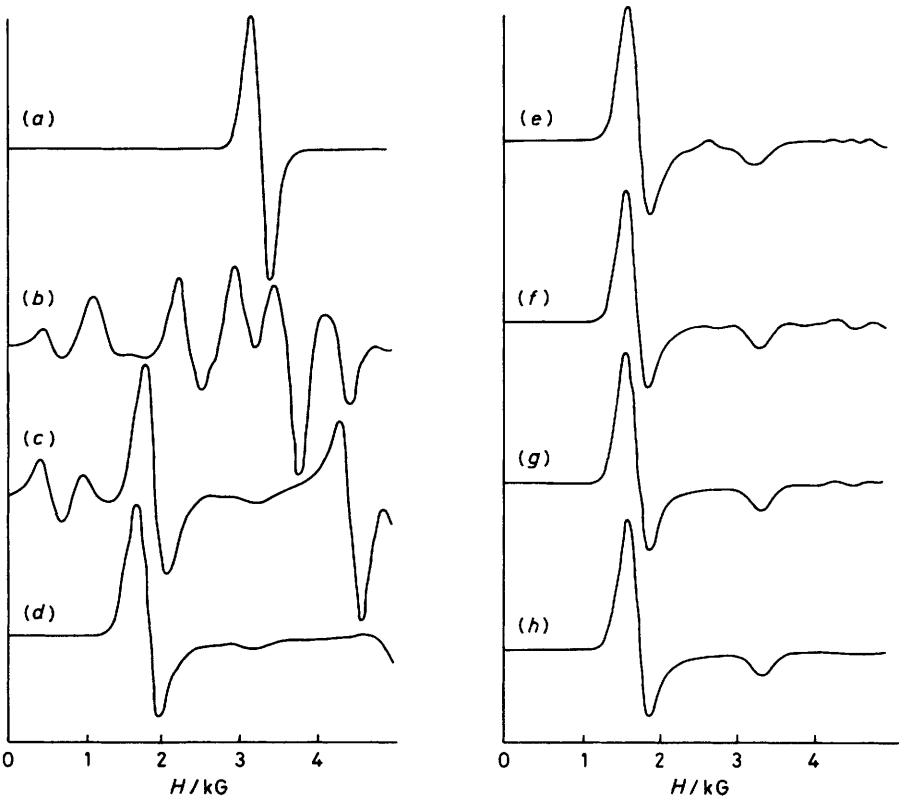

FIGURE 2 Variation with D of the simulated e.s.r. spectra for $S = \frac{3}{2}$, with $\nu = 9.25$ GHz, $g_z = g_x = g_y = 2.0$, $E = 0.0$ cm^{-1}, $W_z = W_x = W_y = 250$ G, dθ = 3°; $D = 0.0$ (*a*), 0.1 (*b*), 0.2 (*c*), 0.3 (*d*), 0.4 (*e*), 0.6 (*f*), 0.8 (*g*), 1.00 cm^{-1} (*h*)

* Throughout this paper: 1 G = 10^{-4} T.

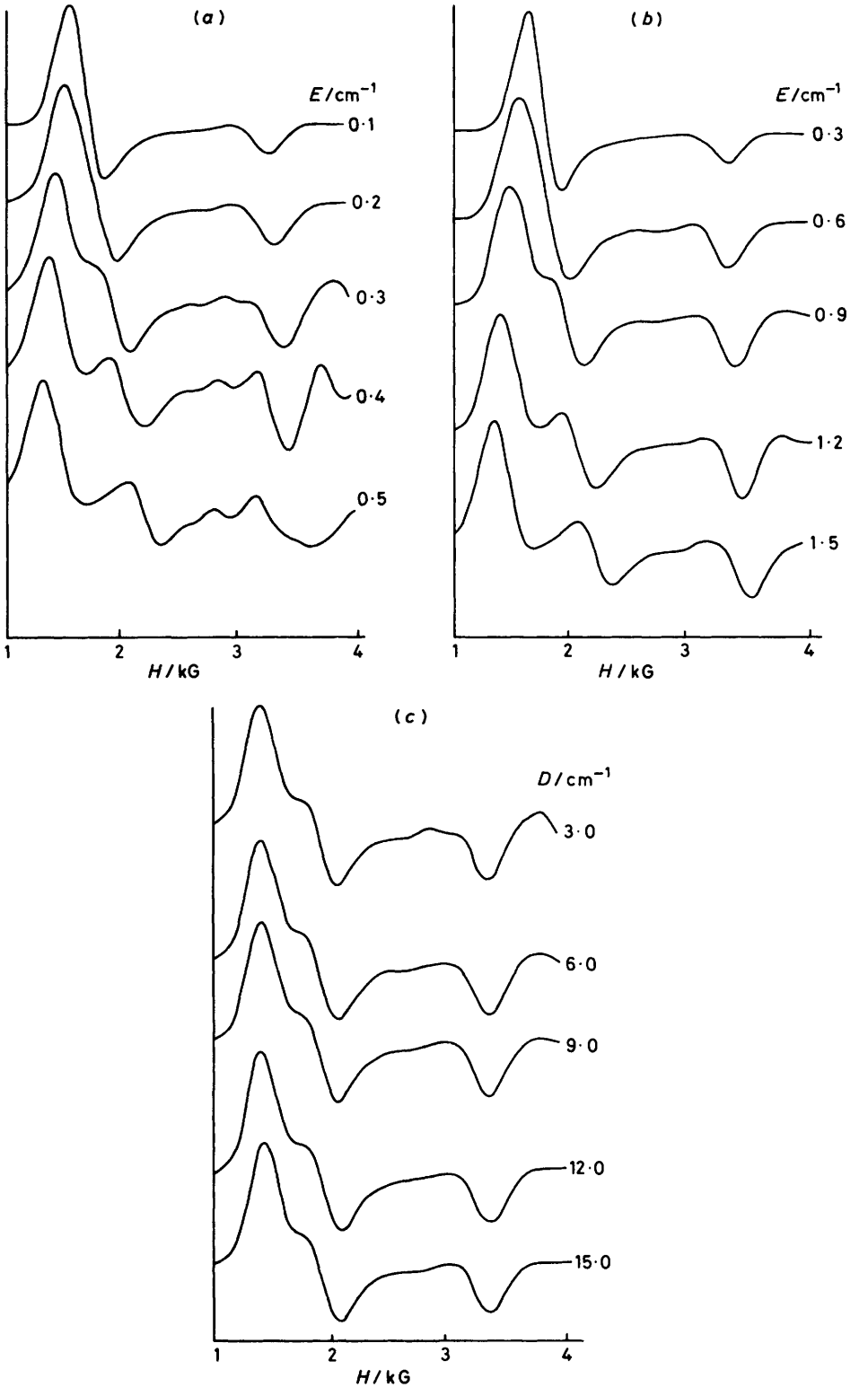

FIGURE 3 Variation with E of the simulated e.s r. spectra for $S = \frac{5}{2}$ with $\nu = 9.25$ GHz, $g_z = g_x = g_y = 2.0$, $W_z = W_x = W_y = 250$ G, $d\theta = 3°$; $D = 3.0$ (*a*), $D = 9.0$ cm^{-1} (*b*), $E = 0.1D$ (*c*)

Simulated E.S.R. Spectra of $S = \frac{3}{2}$ Systems, the Iron–Molybdenum Protein, and Iron–Molybdenum Cofactor of Nitrogenase.—The $S = \frac{3}{2}$ spin state appears to be very important in many iron–sulphur proteins and their synthetic analogues. Thus the effects on the simulated spectra of changing the spin-Hamiltonian parameters are of interest and are briefly illustrated in Figures 2 and 3, assuming typical X-band microwave frequencies *i.e.* $h\nu \approx 0.3$ cm^{-1}. Figure 2 illustrates the effect of increasing D assuming isotropic g values. In this situation all the e.s.r. transitions are coincident when $D = 0$. As D is increased the complexity of the spectra increase until $D > h\nu$, at which stage there are only two features in the most commonly reported magnetic field range (0—5 kG). If numerical values of D and E are required it is essential to obtain spectra over as wide a magnetic field range as possible since resonances may still be observed above 5 kG. In an axially symmetric system when $|D| \gg h\nu$, the low field resonance corresponds to $2g_{\perp}$.[11]

In a system of rhombic symmetry the inequivalence of the principal magnetic axes may be introduced into the spin-Hamiltonian by having $g_x \neq g_y$ and/or $E \neq 0$. We can examine the following two limiting situations: (*i*) $E \neq 0$, but $g_x = g_y$. This is illustrated in Figure 3, for $D \geqslant h\nu$. The main effect, as E increases relative to D, is to eventually split the low field resonance into two components and when $E \geqslant ca.\ 0.1 \times D$, weak, formally forbidden resonances appear to a higher magnetic field. The positions of the resonance fields as a function of D/E when the applied magnetic field is parallel to the molecular axes are shown in Figure 4. The probability of the $\frac{3}{2} \longleftrightarrow -\frac{3}{2}$ transition is zero for $\theta = 0$ and $E = 0$. However, when $E \neq 0$ the probability is no longer zero at this orientation. Thus the appearance of a weak feature to low field of the strong low field resonances definitely shows that $E \neq 0$.

(*ii*) $E = 0$, but $g_x \neq g_y$. In this case the resonance fields of the allowed transitions are given by $H_x = h\nu/2g_x\beta$ and $H_y = h\nu/2g_y\beta$. Hence in this limit any splitting of the low field resonance is caused by g value anisotropy.

These simulations show that for an $S = \frac{3}{2}$ spin state the powder or frozen glass spectra may consist of a large number of features. However, when $D \gg h\nu$ the spectra simplify, see Figure 3, and resemble those observed for FeMo protein and FeMo cofactor, which are typical $S = \frac{3}{2}$ powder spectra under these conditions.

The e.s.r. spectra of both the FeMo protein [2,25] and the FeMo cofactor [2] of nitrogenases from various sources have been interpreted as arising from species with $S = \frac{3}{2}$. The spectrum for FeMo protein has been interpreted by Münck *et al.*[25] on the basis of $g_0\beta_e H < |\Delta|$, where Δ is the zero-field splitting, assuming isotropic g values equal to 2.0 and only considering transitions which occur when the applied magnetic field is parallel to the principal axes. This gave $E/D = 0.055$ whilst the variation in signal intensity with temperature leads to $\Delta = 10.4$ cm^{-1}. We have simulated the FeMo protein spectrum [2] as confirmation of the interpretation as $S = \frac{3}{2}$. However, it must be stressed that the available data cannot be interpreted with a unique set of parameters; we present simulated spectra from the two limiting cases discussed above. For $E = 0$ the spectrum can be simulated with $g_z = 2.00$, $g_x = 1.75$, $g_y = 2.03$, $D = 8$ cm^{-1}, $E = 0$ cm^{-1}, $W_z = 35.0$, $W_x = 50.0$, and $W_y = 50.0$ G; see Figure 5(*a*). In the other limit the spectrum can be simulated,

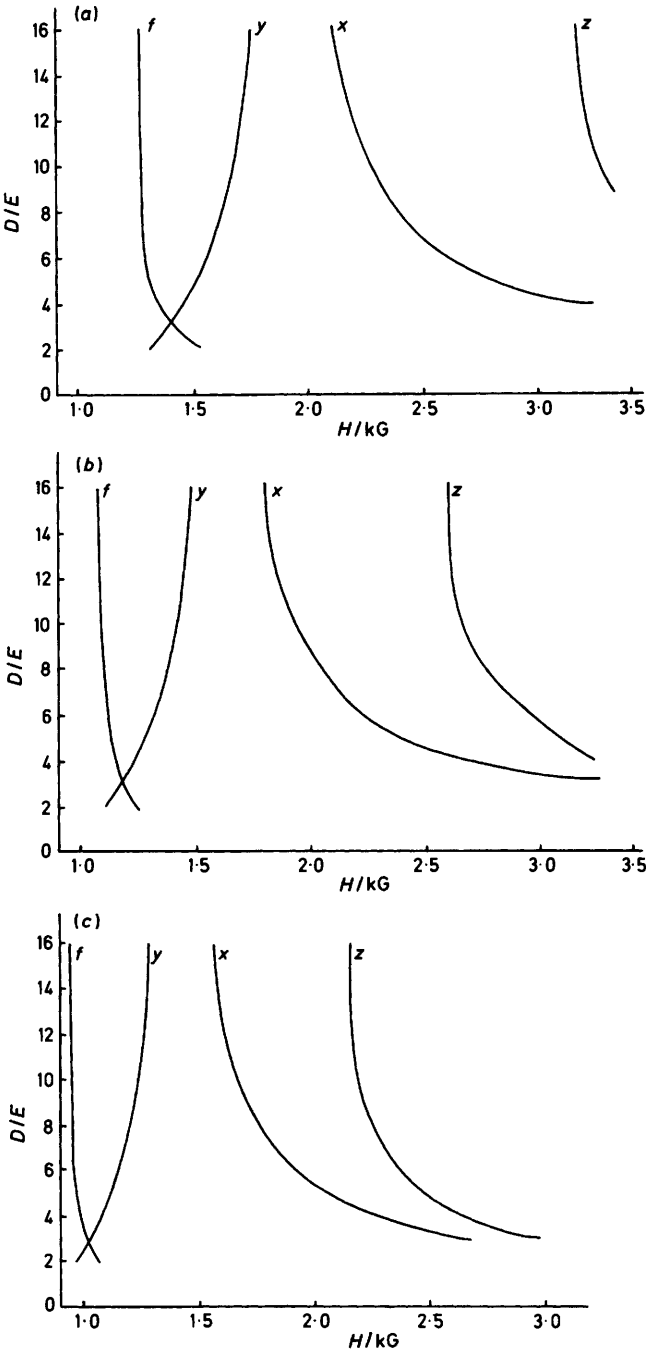

FIGURE 4 Variation of the axis resonance fields with D/E for $S = \frac{3}{2}$, $g_z = g_x = g_y = 1.70$ (*a*); 2.00 (*b*); 2.30 (*c*); for $D \gg h\nu$. *f* Represents a formally forbidden transition

Figure 5(*c*), with $g_z = 2.00$, $g_x = g_y = 1.92$, $D = 8$ cm^{-1}, $E = 0.45$ cm^{-1}, $W_z = 35.0$, $W_x = 50.0$, and $W_y = 50.0$ G. For clarity of presentation the spectra are displayed with the baselines displaced. Apart from small differences in amplitudes the spectra are superimposable. Because of the lack of data at magnetic fields greater than 4 kG it is not possible to define the spin-Hamiltonian parameters more closely. It is worth noting however that in the second simulation the value of $E = 0.45$ cm^{-1} is approaching the upper limit of E in this situation, since for larger values the formally forbidden $+\frac{3}{2} \leftrightarrow -\frac{3}{2}$ resonance at *ca.* 1 100 G aquires significant intensity which is absent in the experimental spectrum.

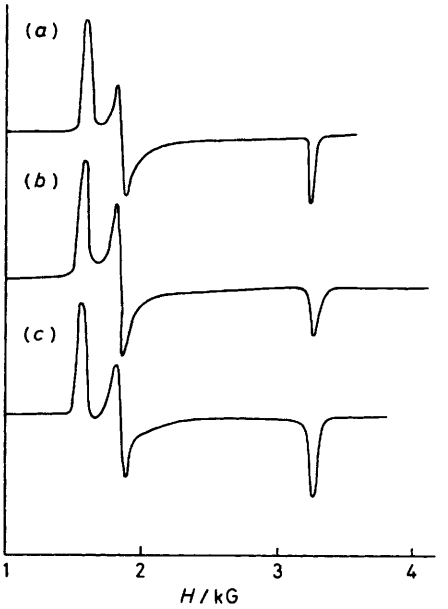

FIGURE 5 Experimental and simulated e.s.r. spectra for FeMo protein of *Azobacter vinelandii* at 13 K. (*a*) Simulation for $S = \frac{3}{2}$ with $g_z = 2.00$, $g_x = 1.75$, $g_y = 2.03$, $D = 8.0$ cm^{-1}, $E = 0.0$ cm^{-1}, $W_z = 35.0$ G, $W_x = W_y = 50.0$ G, $d\theta = 0.5°$; (*b*) experimental spectrum from ref. 2; (*c*) simulated for $S = \frac{3}{2}$ with $g_z = 2.00$, $g_x = g_y = 1.92$, $D = 8.0$ cm^{-1}, $E = 0.45$ cm^{-1}, $W_z = 35$ G, $W_x = W_y = 50$ G, $d\theta = 0.5°$

The experimental spectra of FeMo cofactor resemble that of FeMo protein with the following differences: (*a*) the main features are broadened; (*b*) the resonance positions are shifted relative to FeMo protein; (*c*) there is a weak temperature dependent resonance at *ca.* 1 100 G; (*d*) there is a sharp resonance line slightly on the low field side of $g = 2$, which was attributed to a paramagnetic impurity unrelated to the cofactor.[2]

If the weak temperature dependent resonance at *ca.* 1 100 G is attributed to the $m_s = \frac{3}{2} \leftrightarrow m_s = -\frac{3}{2}$ transition of a $S = \frac{3}{2}$ spin system then clearly $E \neq 0$, although the intense features may still be simulated with $E = 0$, see Figure 6(*a*). A good simulation of the whole spectrum, and that of FeMo cofactor from *Clostridium pasteurianum* at 13 K, has been accomplished, Figure 6(*c*), when $E \neq 0$ with the parameters shown in the Figure. The choice of $D = 8$ cm^{-1} was dictated by both the disappearance of the resonance at *ca.* 1 100 G on changing the temperature to 4.2 K, see Figure 6(*d*)—(*e*), and by the absence of other weak resonances in the magnetic field range reported. The value of E in this limiting situation is determined by the splitting between the two intense low field resonances and by the position and relative intensity of the weak temperature dependent signal. It was found that in order to obtain the correct lineshape for this latter resonance we required a narrower

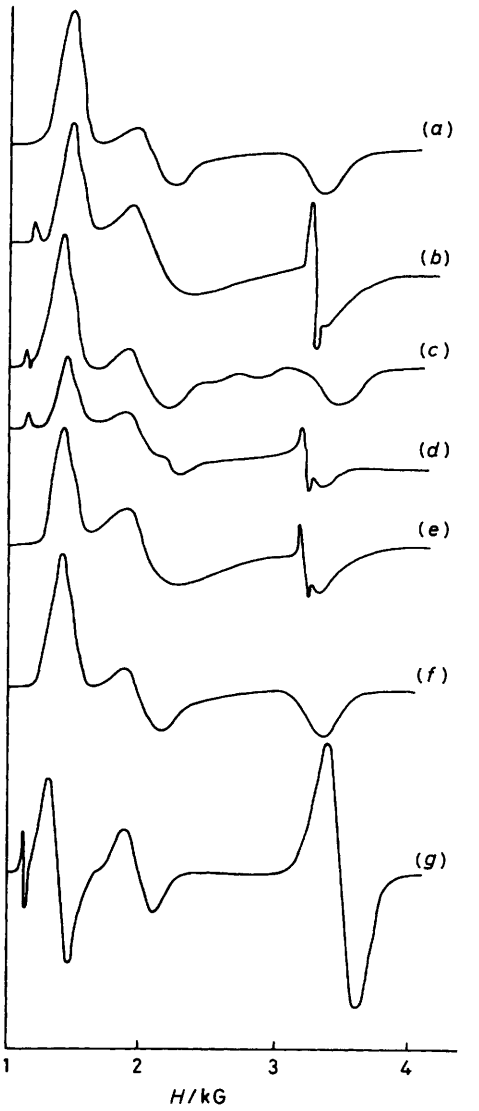

FIGURE 6 Experimental and simulated e.s.r. spectra of FeMo cofactor (*a*) simulated for $S = \frac{3}{2}$ with $g_z = 2.00$, $g_x = 1.60$, $g_y = 2.28$, $D = 8.0$ cm^{-1}, $W_z = W_x = 22$, $W_y = 150$ G, $T = 13.0$ K; (*b*) experimental spectra of *Azobacter vinelandii* at 13 K from ref. 2; (*c*) simulated for $S = \frac{3}{2}$ with $g_z = 1.95$, $g_x = 1.85$, $g_y = 2.10$, $D = 8.0$ cm^{-1}, $E = 0.62$ cm^{-1}, $W_z = W_x = 220$, $W_y = 150$ G, $d\theta = 3°$, $T = 13.0$ K; (*d*) experimental spectrum of *Clostridium pasteurianum* at 13 K from ref. 2; (*e*) experimental spectrum of *Azobacter vinelandii* at 4.2 K from ref. 2; (*f*) simulated for $S = \frac{3}{2}$ with $g_z = 2.00$, $g_x = 1.85$, $g_y = 2.10$, $D = 8.0$ cm^{-1}, $E = 0.62$ cm^{-1}, $W_z = W_x = 220$, $W_y = 150$ G, $d\theta = 3°$, $T = 4.2$ K, computation time 49.2 s; (*g*) simulated for $S = \frac{3}{2}$, using H parallel to molecular axes only with $g_z = 1.90$, $g_x = 1.85$, $g_y = 2.10$, $D = 8.0$ cm^{-1}, $E = 0.62$ cm^{-1}, $W_z = W_x = 220$, $W_y = 150$ G, $T = 13.0$ K

linewidth than that needed for the other transitions. The use of different linewidths for different e.s.r. transitions within an S manifold has been reported previously for Gd^{3+} in rare-earth trifluorides.[26] The larger value of E and the estimated of $\Delta \simeq 23$ cm^{-1} from D and E are

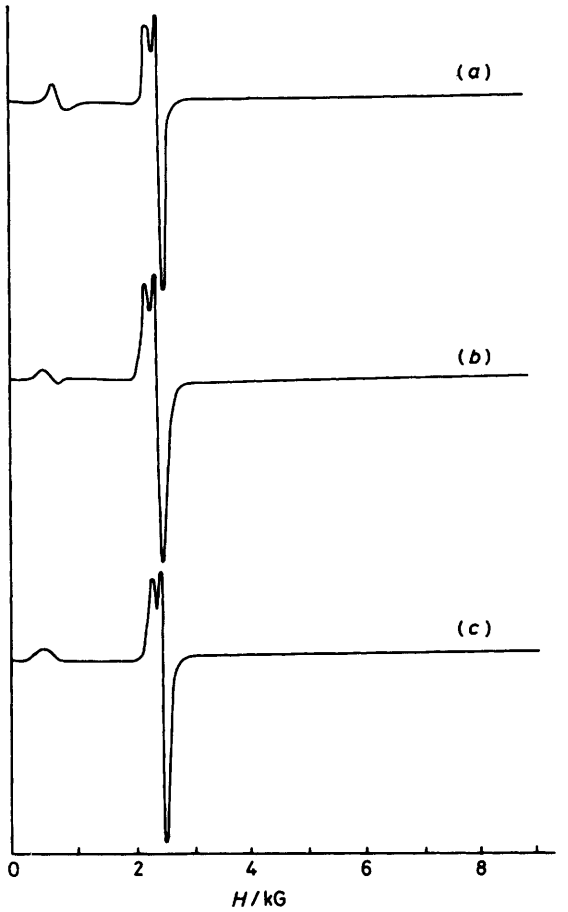

FIGURE 7 Experimental and simulated powder e.s.r. spectra of $[NPr^n_4]_3[Fe_4S_4(SCH_2C_6H_5)_4]$ at 4.2 K: (*a*) simulated at 4.2 K with $g_z = 2.05$, $g_x = g_y = 1.92$, $D = 10.0$ cm^{-1}, $E = 0.0$ cm^{-1}, with $S = \frac{1}{2}$ at zero energy, $\eta = 2$ and $W_z = W_x = W_y = 95$ G and $S = \frac{3}{2}$ at 10.0 cm^{-1}, $\eta = 1$ and $W_z = 300$, $W_x = W_y = 200$ G; (*b*) experimental spectrum from ref. 5; (*c*) simulated at 4.2 K with the parameters in (*a*) except $E = 1.0$ cm^{-1}, computation time 60 s

indicative of a more distorted site in FeMo cofactor than in FeMo protein.

There is the possibility that the weak temperature dependent resonance could arise from a separate species present in low concentrations. Whilst it is not possible to discount this supposition, we feel that the successful simulation of the whole spectrum, and its temperature variation, lends strong support for the view that the whole spectrum does indeed originate from an $S = \frac{3}{2}$ species which is in an environment of rhombic symmetry.[2,25]

The likelihood that the e.s.r. spectrum of FeMo cofactor arises from spin states other than $S = \frac{3}{2}$ has been considered, especially $S = \frac{5}{2}$. However, we have been unable to simulate satisfactorily the spectra on this basis.

Powder E.S.R. Spectra of some $[Fe_4S_4(SR)_4]^{3-}$ *Clusters.*—Holm and co-workers [5] have recently reported the preparation and characterisation of a variety of cubane-like cluster compounds of formula $[NR'_4]_3[Fe_4S_4(SR)_4]$. The e.s.r. spectra of frozen solutions of these species were reported to be compatible with an $S = \frac{1}{2}$ spin system which is either axial or isotropic depending upon solvent conditions. However, in the solid state the compounds exhibited e.s.r. spectra which arose from either (*a*) axially symmetric $S = \frac{1}{2}$ systems with an additional weak resonance at *ca.* 1 500 G, or (*b*) systems with $S > \frac{1}{2}$ and with resonances throughout the region 0—10 000 G (at *X*-band frequencies). However, no detailed interpretations of these spectra have been reported. It became apparent from our simulations of the e.s.r. spectra of FeMo cofactor that at least some of the components of the category (*b*) spectra were characteristic of $S = \frac{3}{2}$ spin systems with $D > h\nu$. This agrees with the interpretation of magnetisation data for $[NEt_4]_3[Fe_4S_4(SCH_2C_6H_5)_4]$ where the magnetic moment tends to that expected for an $S = \frac{3}{2}$ ground state, but with excited states of higher spin multiplicities.[27] Further, the occurrence of the weak feature at *ca.* 1 500 G in the category (*a*) spectra (above) suggested the participation of an additional $S = \frac{3}{2}$ component. We therefore present here the simulation of the polycrystalline e.s.r. spectra of the one category (*a*) and the three different category (*b*) compounds that have been reported.[5]

$[NPr^n_4]_3[Fe_4S_4(SCH_2C_6H_5)_4]$. The experimental spectrum which is typical of category (*a*) compounds is shown in Figure 7(*b*). The main features of the spectrum undoubtedly arise from an $S = \frac{1}{2}$ species. However, magnetic susceptibility measurements [5] strongly suggest that this spin doublet arises from antiferromagnetic exchange interactions within the cubane cluster. Thus the possibility of thermal population of other spin states exists. In the absence of data on the temperature variation of the e.s.r. spectra we have simply empirically weighted the contribution to the simulated e.s.r. spectra of the various spin states, by a factor η, until a satisfactory fit was obtained.

The simulation of the spectrum assumed contributions from $S = \frac{1}{2}$ and $S = \frac{3}{2}$ spin states. For axial symmetry, and assuming each spin state to have the same g values, the simulated spectrum is that in Figure 7(*a*). The simulation of the major $S = \frac{1}{2}$ part of the spectrum is, as expected, extremely good but that for the weaker $S = \frac{3}{2}$ component is less satisfactory. It occurs at too high magnetic field in the simulated spectrum. If we maintain the concept of the g values for each spin state being identical, an almost perfect fit was obtained by allowing the system to be rhombic by having $E \neq 0$, see Figure 7(*c*). Thus, although the spectrum has the appearance of that expected for an axially symmetric system our simulations suggest that it may, in reality, arise from a species with some rhombic distortion.

$[NEt_4]_3[Fe_4S_4(SCH_2C_6H_4OMe\text{-}p)_4]$. The powder e.s.r. spectrum at 4.2 K of this compound,[5] Figure 8(*a*), is similar to that of FeMo cofactor at the same temperature.

The major difference is the weak feature at *ca.* 4 500 G. The observed spectrum can be successfully simulated on the basis of a rhombic $S = \frac{3}{2}$ system, see Figure 8(*b*). The small sharp feature superimposed on the feature between 3 and 4 kG is attributed to an impurity.[5]

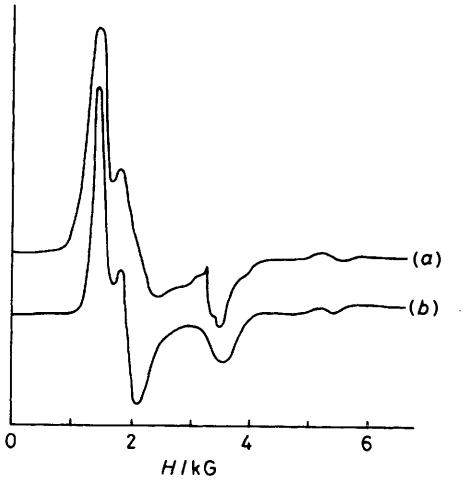

FIGURE 8 Experimental and simulated powder e.s.r. spectra of $[NEt_4]_3[Fe_4S_4(SCH_2C_6H_4OMe\text{-}p)_4]$ at 4.2 K: (*a*) experimental spectrum from ref. 5; (*b*) simulated for $S = \frac{3}{2}$ with $g_z = 2.00$, $g_x = 1.96$, $g_y = 2.10$, $D = 6.0$ cm^{-1}, $E = 0.45$ cm^{-1}, $W_z = 430$, $W_x = 240$, $W_y = 200$ G, $d\theta = 3°$. Computation time 122 s

$[NEt_4]_3[Fe_4S_4(SCH_2C_6H_5)_4]$. The appearance of the e.s.r. spectrum of this compound, Figure 9(*a*), coupled with the magnetic susceptibility data [5,27] strongly suggest the spectrum contains contributions from more than one electronic spin state, *S*. For $S = \frac{5}{2}$ with $g = 2$ and $D > h\nu$, the apparent '$g_\perp$' resonance occurs at $3g$. Thus low field resonance (1) has the position and profile consistent with a spin sextet. However we have been unable to simulate satisfactorily the spectrum assuming only $S = \frac{5}{2}$. The weak feature (2) occurs at a magnetic field compatible with the '$g_\perp$' resonance from $S = \frac{3}{2}$ when $D > h\nu$. Similarly, the broad feature (4) could contain resonances from $S = \frac{1}{2}$. Indeed after many attempts we have found it necessary to include contributions from $S = \frac{5}{2}$, $\frac{3}{2}$, and $\frac{1}{2}$. A satisfactory simulated spectrum involving the superposition of spectra from these three spin states is shown in Figure 9(*b*). The sharp feature (3) has been ascribed to impurities.[5] We have included this possibility in our simulation by adding the spectrum from a further independent $S = \frac{1}{2}$ system, the weighting of which was varied in order to obtain a satisfactory simulation of the spectrum. The simulations were performed assuming axial symmetry. The splitting observed in feature (2), which is not reproduced by the simulation, may be attributed to the presence of a small component of rhombic symmetry. However, in view of the generally good simulation of the spectrum and the lengthy calculation involved we did not consider it worth performing the simulation in rhombic symmetry. This interpretation compares favourably with the magnetisation data [27] in that it involves a $S = \frac{3}{2}$ and a higher lying $S = \frac{5}{2}$ spin state.

$[NMe_4]_3[Fe_4S_4(SC_6H_4Me\text{-}p)_4]$. The powder e.s.r. spectrum of this compound [5] at 4.2 K, see Figure 10(*a*), has the general appearance of a $S = \frac{3}{2}$ system with $D \approx h\nu$. We have been able to simulate most of the spectrum reasonably well on this basis, assuming axial symmetry,

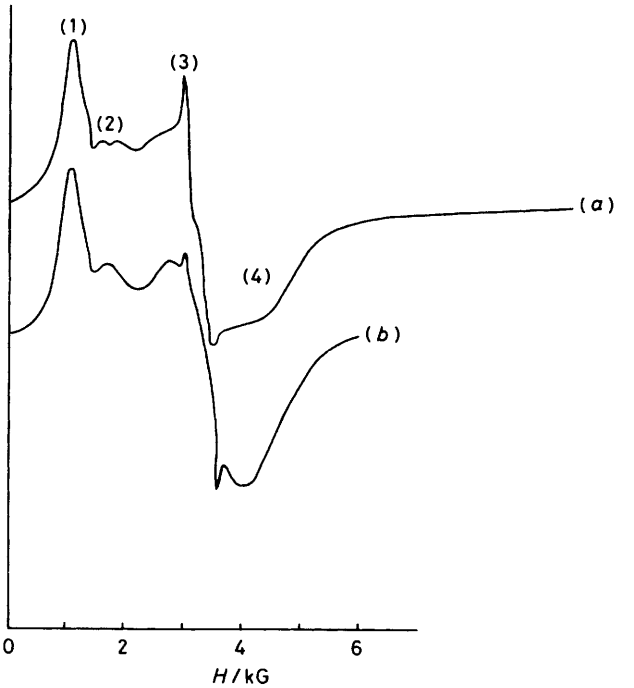

FIGURE 9 Experimental and simulated powder e.s.r. spectra of $[NEt_4]_3[Fe_4S_4(SCH_2C_6H_5)_4]$ at 4.2 K: (*a*) experimental spectrum from ref. 5; (*b*) simulated for $S = \frac{5}{2}$ plus $S = \frac{3}{2}$ and $\frac{1}{2}$ with $g_z = 1.960$, $g_x = g_y = 2.055$, $D = 10$ cm^{-1}, $E = 0$ cm^{-1}, $d\theta = 3°$, $T = 4.2$ K. Linewidths for $S = \frac{5}{2}$, $W_z = W_x = W_y = 400$ G; $S = \frac{3}{2}$, $W_z = W_x = W_y = 1\,000$ G; and $S = \frac{1}{2}$, $W_z = W_x = W_y = 1\,400$ G. Zero-order energies and relative weightings: $S = \frac{5}{2}$ (28, 0.43); $S = \frac{3}{2}$ (10, 0.14); $S = \frac{1}{2}$ (0 cm^{-1}, 1). In addition an $S = \frac{1}{2}$ impurity signal with $g_z = 2.30$, $g_x = g_y = 1.96$, $W_z = 70$, $W_x = W_y = 80$ G, and relative weighting 0.0043 is included. Computation time 22.5 s

see Figure 10(*b*). The high *g* values are dictated by the position of the feature centred on *ca.* 1 500 G. The use of $g_\perp < 2.7$ leads to a simulated spectrum with this feature at higher magnetic fields. The value of *D* required is determined mainly by the separation between the weak feature below 1 000 G and that at *ca.* 1 500 G. In addition to these requirements we have found it necessary to assume a greater linewidth for transitions which occur over the magnetic field range 3 000—5 000 G than for those elsewhere, in order to obtain the required spectral profile. Although the simulation does not account for the feature at *ca.* 6 000 G it is the closest that we have been able to achieve from a consideration of any spin states up to and including $S = \frac{7}{2}$. Of the four compounds considered this has been the most difficult to simulate, and is unusual in that considerably greater values of *g* and smaller values of *D* are required compared

to the other compounds. Although the range of examples considered is very limited, it is tempting to attribute this difference to the presence of an aryl thiolate group as opposed to a more alkyl-like thiolate group in the other compounds.

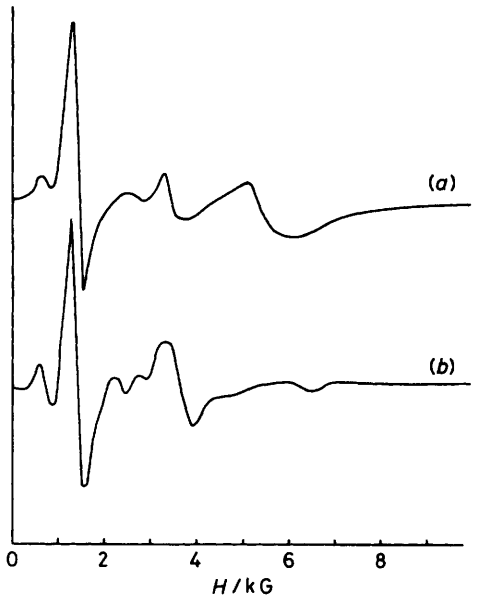

FIGURE 10 Experimental and simulated powder e.s.r. spectra of $[NMe_4]_3[Fe_4S_4(SC_6H_4Me\text{-}p)_4]$ at 4.2 K: (*a*) experimental spectrum from ref. 5; (*b*) simulated for $S = \frac{3}{2}$ with $g_{\parallel} = g_{\perp} = 2.70$, $D = 0.25$ cm^{-1}, $E = 0.0$ cm^{-1}, $W_z = W_x = W_y$ equals 260 G for H in range 0—3 kG; equals 800 G for H in range 3—5 kG; equals 350 G for $H > 5$ kG, $d\theta = 0.5°$. Computation time 75.9 s

The present empirical approach to the interpretation of the e.s.r. spectra of these $[Fe_4S_4(SR)_4]^{3-}$ cubane-like clusters indicates that they may arise from either a single thermally occupied spin state or from a number of closely spaced states which may have different spin multiplicities. The occurrence of an $S = \frac{1}{2}$ ground state in certain of these cluster compounds has been justified using a simple spin coupling model between centres with $S_1 = \frac{5}{2}$, $S_2 = S_3 = S_4 = 2$ spin states and a single isotropic exchange parameter, J.[27] Degeneracies or near degeneracies between different spin states are predicted to occur if coupling between the $S = 2$ centres is allowed to be different to that with $S = \frac{5}{2}$ centres, as expressed in equation (9). This is illustrated in Figure 11 where the relative energies of the lowest spin states are given. These spin states are produced by coupling three tetrahedral Fe^{II} ions together, and then coupling the resultant spins with the spin of the tetrahedral Fe^{III} ion according to the spin-Hamiltonian (9), where centres 1, 2, and 3 are

$$\mathcal{H}_{ex} = -2\alpha J(\hat{S}_1.\hat{S}_2 + \hat{S}_1.\hat{S}_3 + \hat{S}_2.\hat{S}_3) - 2J\hat{S}^*.\hat{S}_4 \quad (9)$$

the iron(II) ions which are coupled[28] to give a set of resultant spins, S^*. The S^* spins are then coupled with the electronic spin, S_4, of the iron(III) ion to give final resultant spins, S'.

We thank the S.R.C. for financial support.

[1/1872 *Received*, 2*nd December*, 1981]

REFERENCES

[1] See for example 'Iron–Sulphur Proteins,' ed. W. Lovenberg, Academic Press, New York, 1977, vols. II and III.

[2] J. Rawlings, V. K. Shah, J. R. Chisnell, W. J. Brill, R. Zimmermann, E. Münck, and W. H. Orme-Johnson, *J. Biol. Chem.*, 1978, **253**, 1001; B. K. Burgess, E. I. Stiefel, and W. E. Newton, *J. Biol. Chem.*, 1980, **255**, 353.

[3] E. J. Laskowski, J. G. Reynolds, R B. Frankel, S. Foner, G. C. Papaefthymiou, and R. H. Holm, *J. Am Chem. Soc.*, 1979, **101**, 6562.

[4] J. W. McDonald, G. D. Friesen, and W. E. Newton, *Inorg. Chim. Acta*, 1980, **46**, L79.

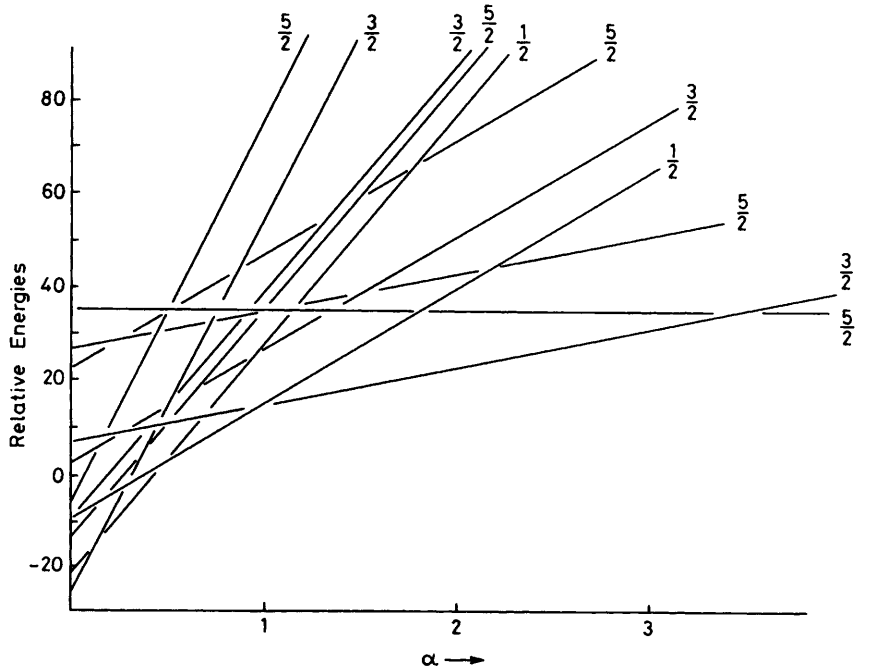

FIGURE 11 Variation with α of the relative energies of the lowest lying spin states derived from equation (9)

[5] T. E. Wolff, J. M. Berg, C. Warrick, K. O. Hodgson, R. H. Holm, and R. B. Frankel, *J. Am. Chem. Soc.*, 1978, **100**, 4640.
[6] C. D. Garner, S. R. Acott, G. Christou, D. Collison, F. E. Mabbs, and R. M. Miller, 4th International Symposium on Nitrogen Fixation, Canberra, December 1980; G. Christou, D. Collison, C. D. Garner, F. E. Mabbs, and V. Petrouleas, *J. Chem. Soc., Dalton Trans.*, following paper.
[7] R. D. Dowsing and J. F. Gibson, *J. Chem. Phys.*, 1969, **50**, 294.
[8] R. Henderson, J. E. Wertz, T. P. P. Hall, and R. D. Dowsing, *J. Phys. C*, 1971, **4**, 107.
[9] R. Aasa, *J. Chem. Phys.*, 1970, **52**, 3919.
[10] A. Abragam and B. Bleaney, 'Electron Paramagnetic Resonance,' Clarendon Press, Oxford, 1970.
[11] B. R. McGarvey, 'Transition Metal Chemistry,' ed. R. L. Carlin, Edward Arnold Ltd., London, 1966, vol. 3, p. 89.
[12] M. J. Nilges and R. L. Belford, *J. Magn. Reson.*, 1979, **35**, 259.
[13] W. Low, 'Paramagnetic Resonance in Solids,' Suppl. 2, Academic Press, New York and London, 1960.
[14] L. S. Singer, *J. Chem. Phys.*, 1955, **23**, 379.
[15] F. G. Wakin and A. W. Nolle, *J. Chem. Phys.*, 1962, **37**, 3000.
[16] F. Holuj, *Can. J. Phys.*, 1966, **44**, 503.
[17] M. Ya Shcherbakova and V. E. Istomin, *Phys. Status Solidi B*, 1975, **67**, 461.
[18] J. R. Pilbrow, *J. Magn. Reson.*, 1978, **31**, 479.
[19] L. E. Mohrmann, jun., and I. B. B. Garrett, *J. Chem. Phys.*, 1970, **52**, 535.
[20] W. V. Sweeney, D. Conconvanis, and R. E. Coffman, *J. Chem. Phys.*, 1973, **59**, 369.
[21] K. Balasubramanian and L. R. Dalton, *J. Magn. Reson.*, 1979, **33**, 245.
[22] C. W. Clenshaw, 'Mathematical Tables,' HMSO, London, 1962, vol. 5; *Math. Tables Aids Computation*, 1955, **9**, 118; M. G. Cox, 'Software for Numerical Mathematics,' ed. D. J. Evans, Academic Press, London, 1974; M. G. Cox and J. G. Hayes, Report NAC26, National Physical Laboratory, Teddington, Middlesex, 1973; W. M. Gentleman, *Comput. J.*, 1969, **12**, 160.
[23] G. D. Simpson, R. L. Belford, and R. Biagioni, *Inorg. Chem.*, 1978, **17**, 2424.
[24] H. Abe and J. Shimada, *Phys. Rev.*, 1953, **90**, 316.
[25] E. Münck, H. Rhodes, W. H. Orme-Johnson, L. C. Davies, W. J. Brill, and V. K. Shah, *Biochim. Biophys. Acta*, 1975, **400**, 32.
[26] V. K. Sharma, *J. Chem. Phys.*, 1971, **54**, 496.
[27] G. C. Papaefthymiou, R. B. Frankel, S. Foner, E. J. Laskowski, and R. Holm, *J. Phys. Colloq. (Fr.)*, 1980, **41**, C1-493.
[28] F. E. Mabbs and D. J. Machin, 'Magnetism and Transition Metal Complexes,' Chapman and Hall, London, 1973, ch. 7.